Challenges in current slope stability analysis methods

Loren J. Lorig
Itasca S.A.

Abstract

Slope stability analysis involves comparison of disturbing forces, due to gravity and water pressure, to the available strength of the rock mass. Such analyses traditionally have been performed using limit equilibrium methods, but currently are frequently carried out using numerical models. It has been suggested that the numerical models do not require further development to meet the needs of slope stability analysis. While this may be true, there are significant challenges in the routine use and interpretation of existing models. These challenges relate to several important uncertainties, including rock mass strength, water pressures and property variability. This paper discusses each of the challenges in some detail and proposes methods to help overcome them.

INTRODUCTION

Present rock-slope design practice is to divide a slope into geotechnical units, each of idealized constant properties, with similar idealization of large-scale discontinuities, into discrete features of specified location and constant properties. Rock mass properties typically are estimated using rock-mass classifications schemes and empirical relations. Water pressures are specified based on assumed phreatic surfaces or, more recently, on flow analyses. Both mechanical and flow analyses are performed separately (often by different professional groups) and, for convenience, both groups ignore all but the largest discontinuities. This conventional practice is combined with admissible safety factors also established essentially by experience. The combined investigation, analysis and acceptable safety factors define a calculation methodology.

The safety factor analyses traditionally have been performed using limit equilibrium methods, but currently are carried out using numerical models. It was suggested almost a decade ago that the numerical models did not require further development to meet the needs of slope stability analysis at the time. However, today there are significant challenges in the routine use of existing models. The challenges relate to several important uncertainties, including rock mass strength, water pressures and property variability.

- **Rock mass strength** — Continuum shear-strength criteria (such as Hoek-Brown) typically are used to describe the shear strength of a rock mass composed of intact material and discontinuities. Among other things, uncertainty with respect to scale effects and values to assign to the disturbance factor, D, in the Hoek-Brown criterion has raised considerable debate among practitioners.
- **Water pressure** — The challenge with water concerns the pressures acting on various components of the rock mass. Typical continuum flow analyses often are calibrated to measured pressures that likely represent the pressures in the more transmissive structures and may not represent the pressures in less permeable parts of the rock mass. Direct application of water pressures from such analyses in stability assessments ignores coupled hydro-mechanical effects, and is equivalent to assuming that the slope is composed of a highly porous and permeable material such as a clean sand or gravel.
- **Variability** — Rock is intrinsically variable in its properties. Similarly, the discontinuities present in any rock mass also are variable with regard to their properties. This variability always shows up as a distribution of values from any site characterization program, and leads to a question regarding the particular values that should be chosen for stability analysis and how results should be interpreted.

This paper will discuss each of the challenges in more detail and propose methods to overcome them.

THE ROCK-MASS STRENGTH CHALLENGE

Current analysis methods involve the use of empirical relations to estimate rock mass modulus and shear strength through one of several rock-mass rating techniques. Discontinuity behavior also usually is derived via empirical relations. This section of the paper focuses on the current and future methods of estimating rock mass strength.

Inherent deficiencies in all empirically derived rock-mass strengths have led to the development of a Synthetic Rock Mass (SRM) approach. However, routine application of SRM methodology is still a ways off, and empirical relations likely will be used for a time.

The most widely used method based on the Hoek-Brown criterion is discussed in detail. Most practitioners agree more or less on the procedures to estimate the parameters required for its use. However, there is considerable disagreement among practitioners with respect to the scale factor which may be related to the disturbance factor, D. The value selected for D can have a significant impact on results. There is a critical need for more guidance regarding this parameter.

Rock-Mass Rating Techniques

Systems of rock-mass rating techniques were developed for use in Civil and Mining Engineering in response to the need for ways to 'rank' a specific rock mass, based, in large part, upon the joints and their weakening effect on rock. Because it is impossible to measure rock mass strength directly, it usually is estimated from empirical relations based on rock-mass rating or classification systems. Rock mass classification is based on systems that assign weighting factors to the values of certain measurable quantities to obtain an overall rating. Classification systems and empirical strength estimates are derived from different environments. Therefore, due to the use of different weighting factors and differences in the 'built-in' experience, there is no one-to-one correspondence between classification systems.

The advantage of these empirical systems is in providing a rapid assessment of rock mass strength that can be used directly in stability (and deformation) assessments. Major weaknesses include the fact that they are not always based on mechanics and that they combine all characteristics into a single number. For example, it is possible to have two rock masses with the same rating but with different behaviors due to variations in discontinuity characteristics — i.e., failure modes cannot be resolved.

Table 1 lists (in chronological order) several of the rock-mass rating techniques. Those in bold allow direct estimation of rock-mass shear strength. In the Q-system, the relation between the Q-rating and rock mass strength is given by an equation developed by Singh & Goel (1). The equation relates rock mass cohesion to the Q-rating and the intact rock density. The most commonly used shear-strength estimation method is based on the Hoek-Brown failure criterion. The evolution of this criterion is discussed in the next section.

Q	Rock Mass Quality	Barton et al. (2)
RMR	**Rock Mass Rating**	**Bieniawski (3)**
MRMR	Mining Rock-Mass Rating	Laubscher (4)
RMS	Rock Mass Strength	Selby (5)
SMR	Slope Mass Rating	Romana (6)
SRMR	**Slope Rock-Mass Rating**	**Robertson (7)**
GSI	**Geologic Strength Index**	**Hoek (8)**
CSMR	Chinese system for SRMR	Chen (9)
RMi	Rock Mass index	Palmstrøm (10)
M-RMR	Modified rock-mass classification	Unal (11)
BQ	Index of rock-mass basic quality	Lin (12)

Table I – Rock-mass rating techniques

Hoek-Brown Criterion

This section discusses the evolution of the Hoek-Brown criterion, particularly with respect to slope stability analysis, and is taken largely from an article by Hoek and Marinos (13). The original Hoek-Brown criterion (Equation 1) was presented by Hoek and Brown (14):

$$\sigma_1 = \sigma_3 + \sqrt{m\sigma_c\sigma_3 + s\sigma_c^2}$$

The criterion was developed to provide input for the design of underground excavations, because no other suitable means existed to estimate rock-mass shear strength. The criterion was based on tests of andesite (UCS = 265 MPa) from the Bougainville open-pit copper mine. The criterion assumed the following:

- rock mass failure controlled by translation and rotation of individual blocks;
- failure of intact rock played no significant role; and
- jointing pattern sufficiently 'chaotic' to assume isotropic behavior.

In 1983, Hoek published equations to relate Φ. and c to the Hoek-Brown criterion. This allowed the criterion to be used in software written in terms of the Mohr-Coulomb criterion. Hoek's 1983 article (15) also provides the most comprehensive discussion of the original Hoek-Brown criterion.

It soon became apparent that the original criterion was too optimistic for slope design. Consequently, the concept of disturbed and undisturbed rock mass was introduced (16) to provide a method for downgrading near-surface rock masses. As will be discussed later, an alternative explanation is that, because slopes typically involve a larger scale than underground excavation, the rock mass appears weaker in slopes than in underground excavations. In addition, a method to estimate Hoek-Brown parameters from Bieniawski's RMR was introduced.

In 1992, the a parameter was introduced so that the modified Hoek-Brown equation produced a criterion with zero tensile strength (17). The resulting relation is shown in Equation (2):

$$\sigma_1 = \sigma_3 + \sigma_{ci} \left(m_b \frac{\sigma_3}{\sigma_{ci}} + s \right)^a$$

By 1994, it was recognized that a system based more heavily on fundamental geological observations and less on blind application of 'numbers' was needed. Hoek (8) introduced GSI as a replacement for Bieniawski's RMR as the principal vehicle for geological data input for the Hoek-Brown criterion. This is a very important consideration, because it forced the user to consider scale effects for the first time. Previously, the same rock-mass strength was estimated for both underground excavations and rock slopes.

In 1997, Hoek and Brown introduced the linear regression method for estimating the equivalent Mohr-Coulomb cohesion, and the friction angle was introduced (18). The most important aspect of this curve-fitting process is to decide the confining stress range over which the linear regression is performed.

In 2002, Hoek et al. (19) provided new derivations of the relations between mb, s, a and GSI. The D parameter also was introduced to account for blast damage (and stress relaxation in slopes). The largest value of D (D = 1) essentially reduces the rock mass cohesion by a factor of two. Again, an alternative explanation is that, because of the scale involved in rock slopes, the rock mass is weaker than that around an underground excavation.

There have been at least three attempts to quantify the Hoek-Brown parameters so that more precise estimates of rock mass strength can be obtained: Douglas (20) described refinements of methods to calculate m_b, s and a based on additional analysis of intact rock tests and limited back-analysis of slopes; Gibson (21) used fracture frequency and joint condition to calculate these same parameters; and Cai et al. (22) used block volume and joint condition factors to calculate GSI. However, none of these 'refinements' addressed the issue of the effect of scale on rock mass strength.

In reviewing the application of the Hoek-Brown criterion in the slope analysis, it is important to recall the following limitations.

• A fundamental assumption of the Hoek-Brown criterion is that the rock mass to which it is being applied is homogeneous and isotropic.
• It should not be applied to the analysis of structurally controlled failures in cases such as hard rock masses, where the discontinuity spacing is similar to the size of the tunnel or slope being analyzed, and where the failure processes are clearly anisotropic.
• The Hoek–Brown criterion is a strength criterion — not a constitutive relation.
• Scale effects are difficult to assess, particularly for large rock slopes.

The third limitation has been addressed by the development of a full constitutive relation (23) based on the Hoek-Brown criterion. Using an appropriate softening relation, the model also can represent the transition between brittle and ductile rock behavior. The flow rule is based on general knowledge of the volumetric behavior of rock, which usually exhibits large dilation at low confining stresses and small, or zero, dilation at large confining stresses.

However, the question of scale effect still remains. Sjöberg (24) and others have highlighted the importance of scale in analysis, as shown in Figure 1. One possible reason for this is the conceptual figure that depicts the conditions under which the Hoek–Brown criterion can be applied (see Figure 2). A different depiction of the rock mass in relation to the scale of the structure being considered highlights the importance of scale. A rock mass that might appear 'blocky' for an underground excavation could appear to be 'disintegrated' for a large slope, as shown in Figure 3. As will be discussed in the next section, the Synthetic Rock Mass (SRM) provides a method for addressing both the problem of anisotropy and the problem of scale effects.
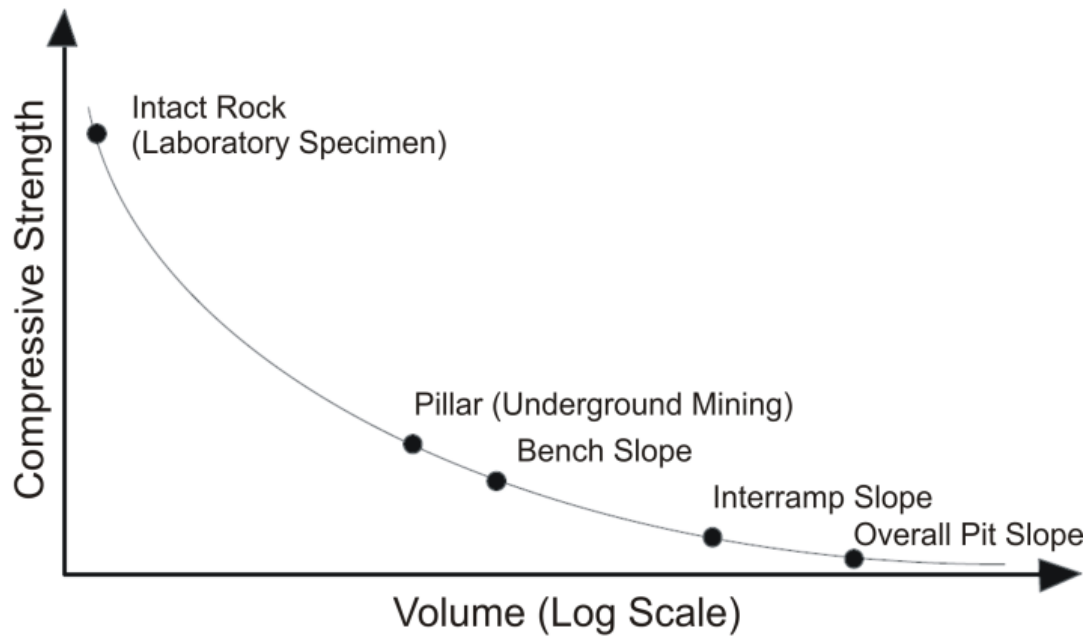
**Figure 1** – *Scale effect on rock-mass compressive strength (24)*
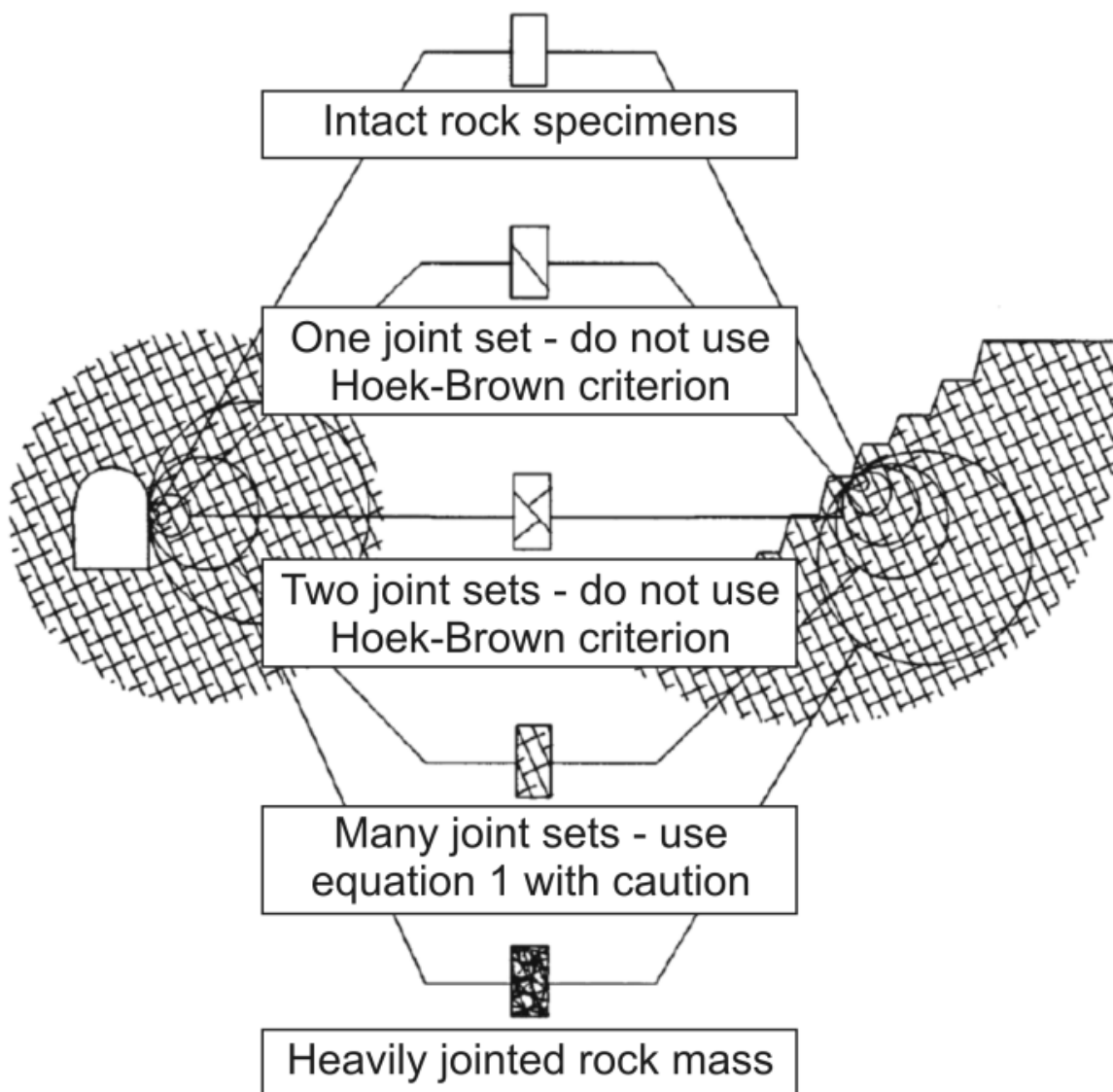
Figure 2 – *Idealized diagram showing the transition from intact to a heavily jointed rock mass with increasing sample size (18)*
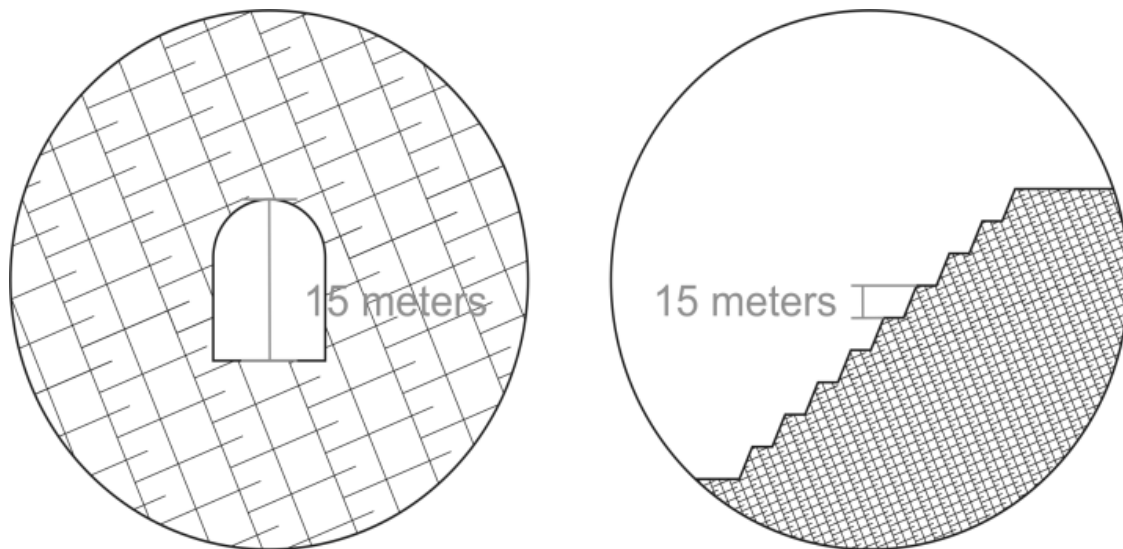
Figure 3 – *Illustration of how the same rock mass could appear 'blocky' for an underground excavation, but 'disintegrated' for a slope*

Synthetic Rock Mass (SRM) Models

SRM models attempt to reproduce the combined effects of intact fracture and discontinuity movement. Main inputs are intact rock properties, joint properties and a Discrete Fracture Network (DFN). SRM models are not new. For example, Carvalho et al. (25) used two-dimensional UDEC (26) models of diorite to estimate rock mass strengths for slope stability studies (see Figures 4 and 5). Worthy of note is the observation that the failure mechanism in the triaxial samples is mainly a consequence of tensile failure of the intact rock bridges in the rock mass.
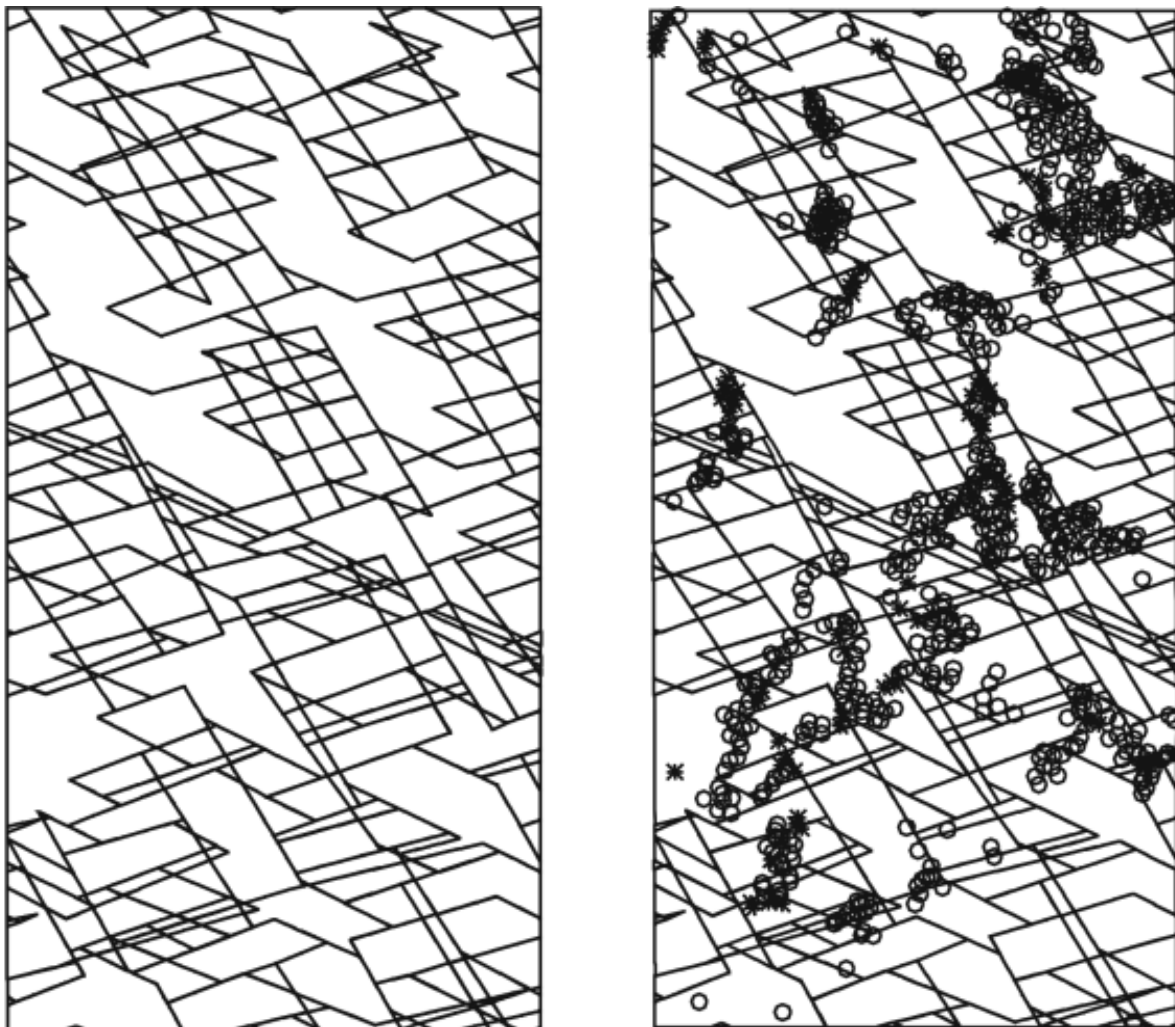
Figure 4 – *Rock mass sample: before (left) and after (right) numerical triaxial test (circles indicate tensile failure locations)*
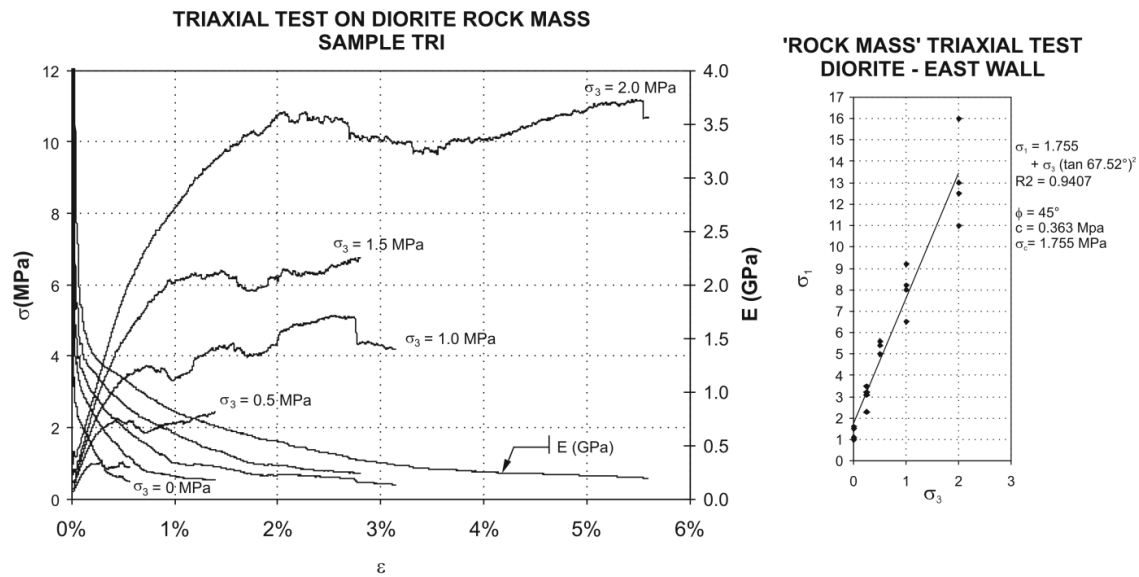
Figure 5 – *Rock mass sample: Stress-strain curves (left) and Mohr-Coulomb envelope (right)*

Clark (27) used FLAC (28) with ubiquitous joints to construct an SRM model. The orientation of the ubiquitous joints was sampled from the actual distribution of joint orientations. The SRM model exhibited anisotropy, scale effects and reasonably reproduced empirical strengths, as shown in Figure 6. Park et al. (29) constructed SRM models with the two-dimensional Particle Flow Code (PFC, 30), as shown in Figure 7. One limitation of this approach is that the joints were 'bumpy', with irregularities of the scale of the individual PFC particles. Recent advances in PFC modeling of SRM models include:

- extension of the modeling to three dimensions;
- a new 'smooth joint' contact model developed to overcome the 'bumpy joint' problem;
- faster model construction [Large-scale 3D models (tens of meters) of up to 1.5 million particles and thousands of discontinuities can be generated in 6–8 hours.]; and
- a more rapid testing methodology. [Currently, UCS testing of SRM models consisting of approximately 5000, 50,000, 500,000 and 1.5 million particles can be performed on the order of an hour, a day, several days and a week or more.]

When setting up the SRM unit, the intact rock properties of the synthetic material are represented by an assemblage of bonded particles calibrated to those measured for an intact sample using a numerical sample with size equal to the average intact-block sizes in the slope being analyzed. These properties typically include measured values of modulus, Poisson's ratio, UCS, tensile strength and fracture toughness. For further information regarding development and application of the SRM technology using PFC refer to (30). In summary, the SRM technique provides a method for integrating the impact of the stochastic nature of the in-situ fracturing, and the strength of the solid rock mass between fractures, into a large-scale model that can be tested in a numerical laboratory to determine rock mass properties without resorting to empirical methods.
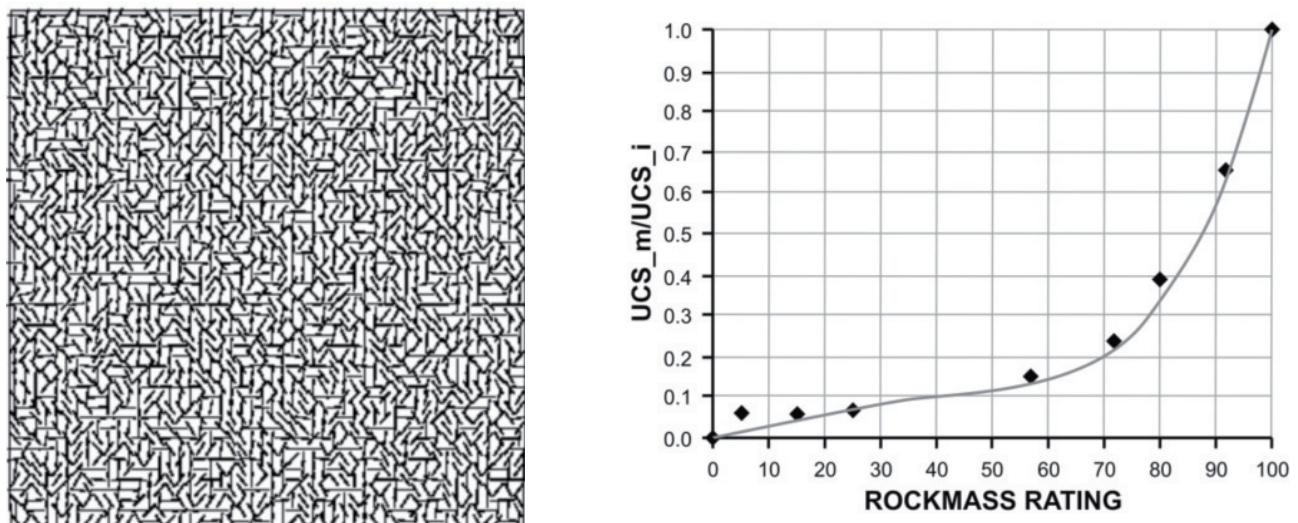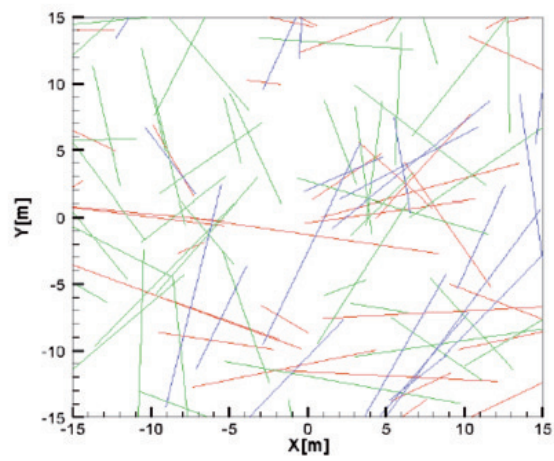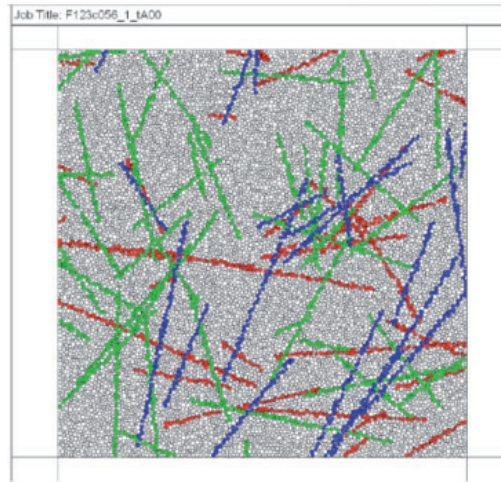

Figure 6 – *FLAC SRM model with four ubiquitous joint sets (top) and the SRM properties (shown as solid markers) compared against the empirical estimate of Barton (32) as cited in Hoek (33), shown as solid line (bottom)*
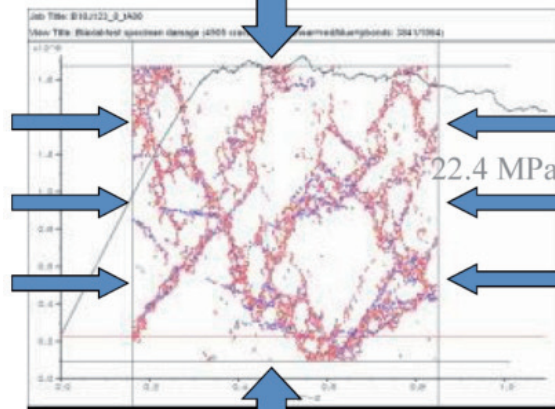
Mapping results

(a)

PFC2D "Sample"

30 meters

(b)

Biaxial test

22.4 MPa

(c)

Figure 7 – *Two-dimensional SRM model with PFC2D with 'bumpy' joints (29)*

New Lattice Models (The Slope Model and BloUp)

The SRM methodology has been extended into a fully three-dimensional numerical model for slope stability analysis, named Slope Model. Rather than using finite-sized PFC particles, greater efficiency is realized with a "lattice" of point masses connected by springs. This model, described by Cundall and Damjanac (34) elsewhere in these proceeding, allows fracture, by breakage of springs and joint slip, using a smooth representation of joint segments.

The lattice formulation of Slope Model is similar to that of the HSBM code BloUp (35), used for simulating the complete blasting process. In particular, the damage induced in a slope near the blast site can be quantified by BloUp in terms of microcracks (broken lattice springs). Figure 8 shows the extent of damage behind a typical blasthole fired 25 ms after the pre-split line. The figure represents a 200-mm diameter blasthole that is 14-m long, and has a charge length of 8 m and stemming of 6 m. The explosive is ANFO at a density of 0.8 g/cc. The rock mass has seven major "medium strength", persistent discontinuities that can be grouped into 3 sets. One sub-vertical set (dip of 55-65), one horizontal (dip of 10) and one vertical (dip of 85). Joints in the current version of HSBM are modeled by weakening the tensile strength of the springs that span the joint surface. In this model, joints have a strength equivalent to 75% of the intact rock value. This is classified in the model as medium strength. The intact rock properties assumed are:

Density= 2200 kg/m^3
Young's modulus = 20 GPa
Poisson's ratio = 0.22
UCS= 50 MPa
tensile strength = 4 MPa
damping = 0.5
Friction angle = 25°

It may be possible (in a future development) to quantify the D-factor discussed above and/or import this damage field into Slope Model in order to include the effect of blast damage on slope stability.
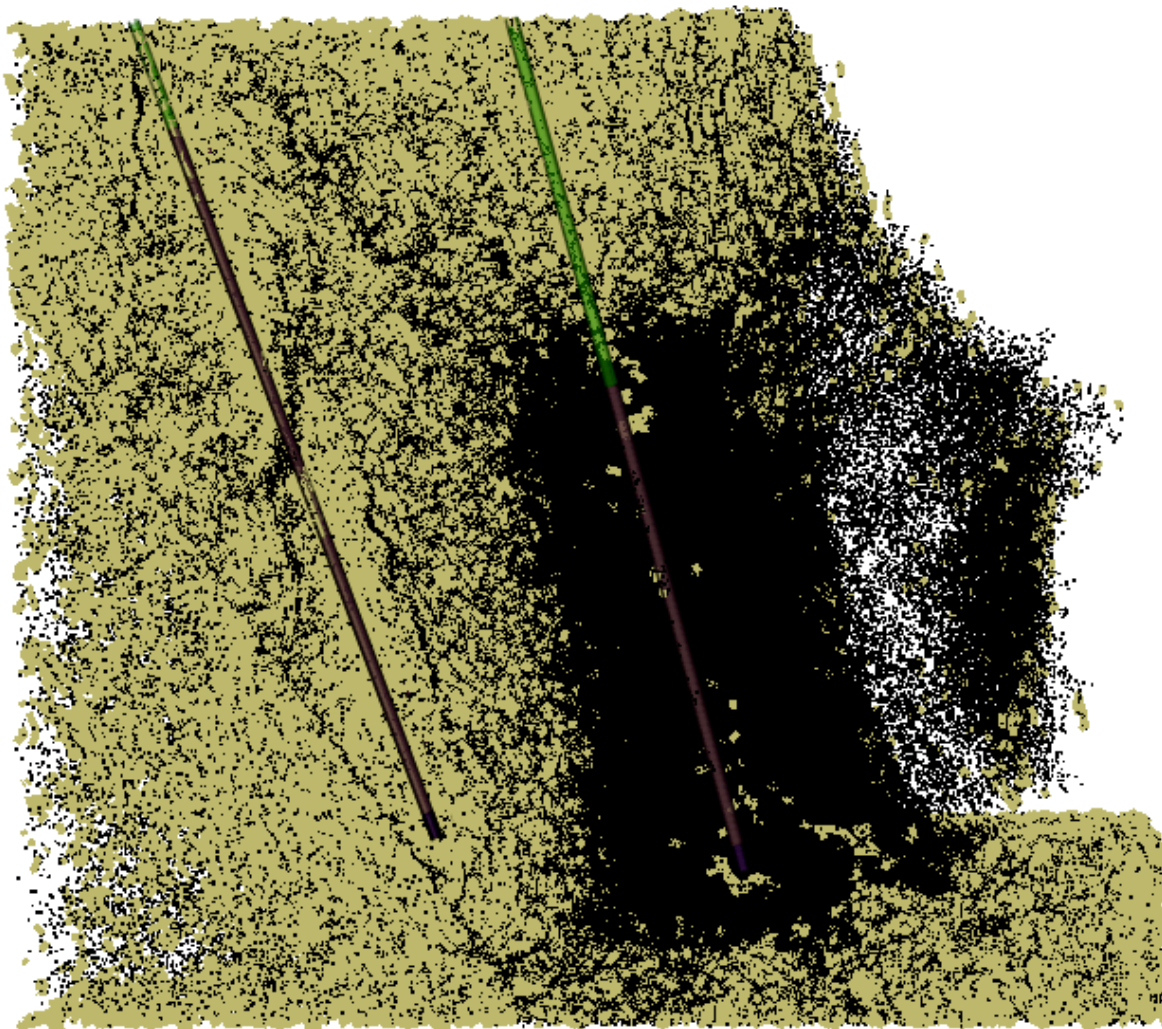
Figure 8 – *BloUp model showing extent of damage behind a typical blasthole fired 25 ms after the pre-split line [Courtesy of HSBM and Italo Onederra]: Black lines indicate fractures in rock.*

THE GROUNDWATER CHALLENGE

The fundamental assumption underlying all stability analyses in jointed and fractured rock slopes with water should be that the effective stress principle applies at all scales of analysis, from large-scale regional faults to microfractures. [In this discussion, any defect in the rock mass that may contain water under pressure is considered to be a discontinuity regardless of scale.] If we assume, for the moment, that there can be no failure of intact rock, then all that is required to perform slope stability analysis is to construct a model that includes all the discontinuities, specify their shear-strength parameters and introduce the water pressure acting on each discontinuity at the time of interest. Of course, this is not practical due to the following.

- The distribution of discontinuities and their strengths are unknown — and probably unknowable.
- Even if we knew the location, orientation and persistence of all the discontinuities, it would be impossible to include them all in any numerical simulation due to limitations in computational speed.
- The distribution of water pressures in discontinuities behind a slope at any particular time generally is not known.

The first two difficulties generally have been addressed by estimating the equivalent shear strength of the rock mass. Because the shear strength of the rock mass cannot be measured directly, it often is estimated empirically. This approach eliminates the need to specify the discontinuities at some analysis scale, as they are considered implicitly in the rock-mass shear strength. In effect, the first two difficulties are handled by treating the rock mass in a manner similar to a soil and replacing the first two difficulties by another — i.e., estimating the rock mass (or equivalent soil) shear strength.

The third difficulty often is addressed by performing some kind of flow analysis, usually employing some form of an equivalent porous-media approach and applying the resultant water pressure distribution to all discontinuities in the mechanical model. [In fact, because the soil mechanics analogy is pervasive, the water pressure in rock slopes usually is called a pore pressure.] The flow analyses typically ignore the potential role of slope deformation in changing water pressures within discontinuities and in changing the conductivity of discontinuities.

In order to better understand the role of slope deformation on water pressures and permeabilities, it is useful to consider two different scenarios. One is a slope excavated in saturated clay. The other is a slope excavated in saturated gravel.

When the saturated clay slope is excavated, the volumetric expansion experienced by the clay near the excavated slope leads to a reduction in pore pressure. The magnitude of the change in pore pressure, Δp, depends on the product of volumetric strain, $\Delta V / V$, and bulk modulus of water, K_w, according to the following expression:

$$\Delta p = \Delta V / V * K_w$$

where ΔV the change in volume of the pore space, and V is the original volume of the pore space.

The bulk modulus of water is typically between 1 GPa and 2 GPa (depending on the amount of entrained air in the water). Because the individual pore spaces in clay are relatively small and the water bulk modulus is much higher than the soil matrix, even a small volumetric expansion leads to significant changes in pore pressure. In clay, the effective stress does not change (because the bulk modulus of water is high compared to that of the matrix). Thus, even vertical slopes in clay can be stable for a period of time. Because the conductivity of clay is typically very low, reduced pore pressures in the clay slope recover extremely slowly. Accordingly, flow analyses seldom are considered for slopes in clay.

Slopes excavated in gravel behave differently. In gravel slopes (and many waste dumps), the original void space is large and well connected. Any change in pore pressure due to slope excavation is lost quickly due to the high conductivity and connectivity of the gravel voids. Accordingly, stability analysis of gravel slopes requires flow analysis (often steady-state) to determine the pore pressure distribution in the slope; deformation analysis almost never is considered.

Real slopes excavated in a saturated discontinuous rock mass do not behave as either clay or gravel, but, as shown later, something in-between. The microfractures in intact rock probably behave more as voids in clay, whereas rock blocks separated by well-connected clean transmissive discontinuities probably behave more as gravel. Complete understanding of the water pressure distribution within a discontinuous rock slope at any particular time requires a coupled mechanical-hydraulic analysis, in which fracture conductivity and pressure are dependent on mechanical deformation, and, conversely, joint water pressures affect the mechanical behavior. It should be noted that the preceding discussion has focused on volumetric deformation. However, shear deformations in a rock mass also introduce volumetric changes due to dilation resulting from shear.

State of Practice

Depending on experience and available analysis tools, practitioners follow a variety of approaches for slope design. These approaches are described below, and range from the simple to complex.

"Dry" Slope Approach — In this approach, the slopes are assumed to be "dry" or "drained". What "dry" means is not always well defined by practitioners. To some, "dry" may mean that water flow and seepage may appear on the slope face, as long as no significant pressures develop within the slope. That is, no water pressure will be present between the slope face and any potential failure surface. In other cases, the practitioner may mean that no water should appear on the face of the slope. In either case, the "dry" slope requirement shifts the responsibility to hydrogeologists, who must provide dewatering measures (e.g., wells and/or horizontal drains) to ensure a "dry" slope. In many cases, no evaluation is made to determine if dewatering can achieve "dry" conditions in the time available.

In evaluating the effectiveness of dewatering measures, the designer or owner may assume the slopes are dry, because only damp spots or minor seeps with negligible flows are seen on existing slopes, drill holes and tunnels. Many times, this assessment ignores the evaporation that can occur, particularly in some low-humidity environments. An auxiliary argument suggests that even if water pressure were present in the slope, slope deformation due to unloading and/or shear dilation at the initiation of slope failure would result in zero water pressure; therefore, the slopes are "dry" for all intents and purposes.

"Wet" Slope Approach — This is probably the most common approach. The approach assumes that the rock mass below the phreatic surface is fully saturated and that water pressure acts on all discontinuities regardless of scale and/or connectivity. Essentially, the slope is assumed to be composed of gravel. However, in almost all cases, the rock mass is represented as an equivalent continuum. Flow analyses often are performed to determine the steady-state distribution of water pressure in the slope. Resultant pressure distributions ignore possible water-pressure reductions due to slope deformation.

It should be noted that the concept of a phreatic surface is not useful in a jointed rock mass with poor connectivity. There are simply water pressures and water content, which may exist in separate regions. A continuous boundary between saturated and unsaturated parts may not exist.

Hybrid Approach — This approach attempts to acknowledge the different water-pressure regimes that can exist within a slope, which is represented as a system of rock blocks separated by explicit discontinuities. The rock blocks typically behave as a continuum that implicitly includes minor discontinuities, and may or may not specify water pressure. (Major discontinuities typically have water pressures specified.) The inherent assumption is that the major discontinuities are transmissive, and often have high conductivity and connectivity such that the water pressure within them is not affected by slope deformation. This assumption is valid as long as the major structure is not clay-filled, as is sometimes the case. The hybrid approach offers the most flexibility, as different water pressures can be specified separately in various components of the rock slope. For example, the major transmissive structures may have 100% of the water pressure found by flow analysis, and the rock mass may have 50% of the water pressure found by flow analysis. The debate over relative percentages stems from the interpretation of monitoring data used to calibrate the flow analysis models.

The "Correct" Approach

Theoretically, back-analysis of slope failures should be capable of identifying the "correct" approach. However, all three approaches described above have met with varying degrees of success in back-analysis of failures. Because, historically, there have been uncertainties regarding both rock mass strength and water pressure distributions, there are many combinations of strength and water pressure that can reproduce slope failures. Therefore, no single approach has been accepted universally. The "correct" approach would seem to be one that accounts for the coupled nature of slopes excavated in jointed rock.

Hydrogeology Basics

Geologic materials have about 13 orders of magnitude range in their hydraulic conductivities, and it is not unusual to have materials differing by 4 orders of magnitude adjacent to each other in a mine area (36). Figure 9 indicates the range of average conductivities based on data from 23 mines. Rock mass conductivity is attributable almost entirely to fractures of different scales, so the range in conductivity is understandable. However, it is reasonable to assume that most calibrated conductivities are based on data attributable to the larger, more transmissive fractures, as smaller fractures contribute little to the overall conductivity.

Storage is the other primary hydraulic property of a geologic material. Specific yield is one type of storage; it is the volume of water that is released by actual drainage of the pores when the phreatic surface is lowered. According to Bear (37), the specific yield (Sy) is equal to the porosity (n) minus the residual moisture content (Cr): $Sy = n - Cr$. Note that Cr varies with time and depends on the previous state of saturation. However, Cr is typically much smaller than n, so that specific yield is approximately equal to porosity. Specific yields for the same 23 mines shown in Figure 9 are shown in Figure 10. It is interesting to note that while rock masses have conductivities similar to soils (especially silts), their porosities are one or two orders of magnitude less. This makes the coupled hydro-mechanical behavior of rock slopes potentially different from that of soil slopes, where hydro-mechanical behavior often is ignored.
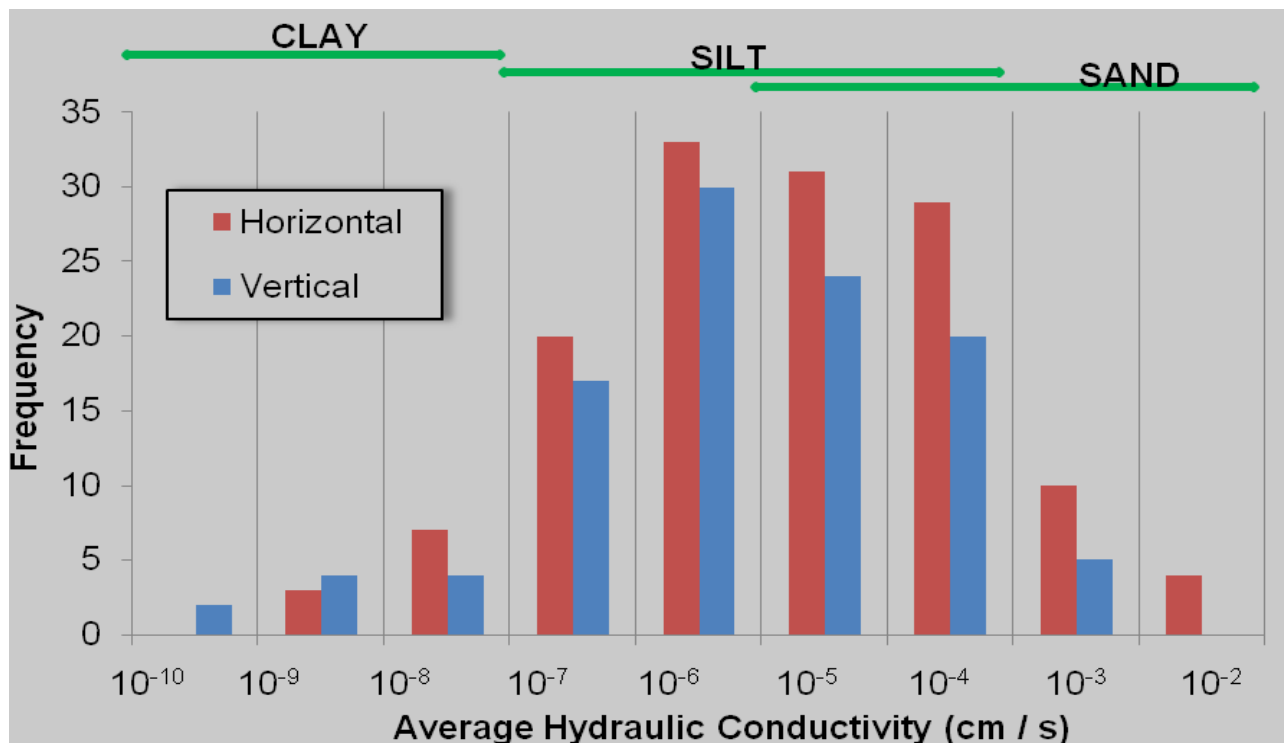
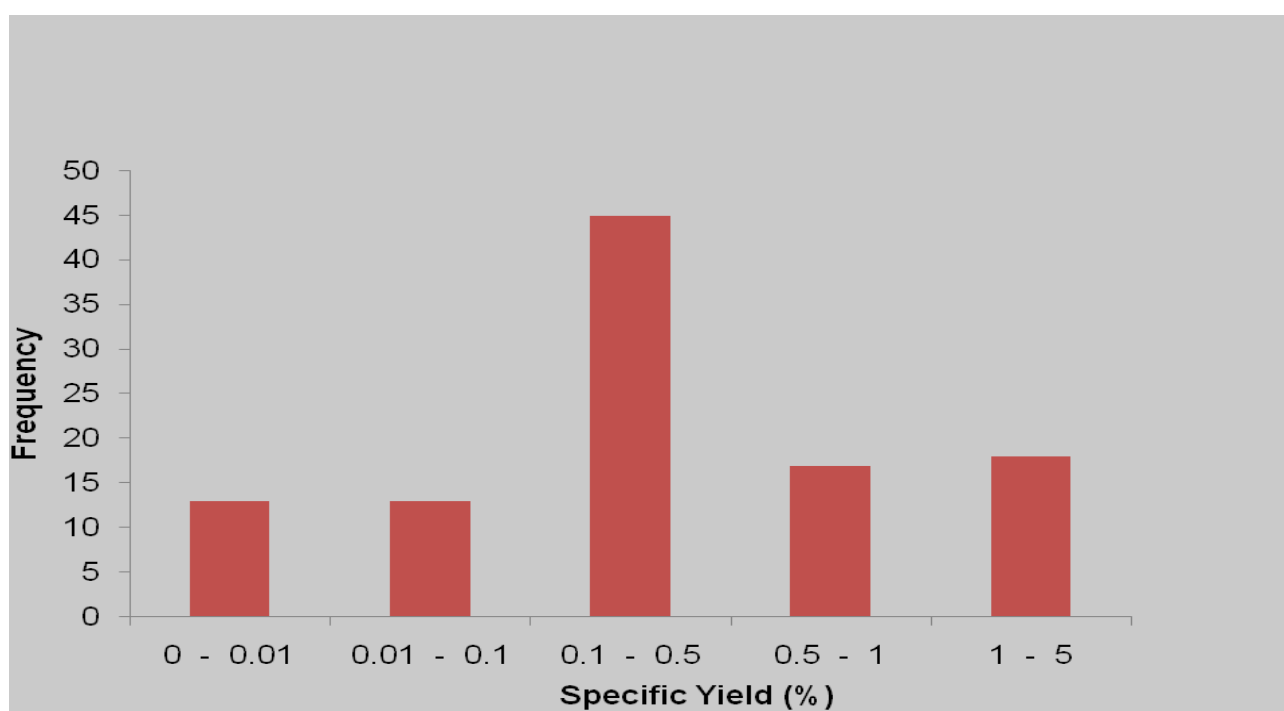*Figure 9* – *Histogram of average hydraulic conductivity from 23 mine sites*

Figure 10 – *Histogram of specific yield from 23 mine sites*

Excavated rock-slope hydraulic behavior can be divided conveniently into two sequential stages — i.e., a poro-elastic (could also be poro-plastic) stage and a transient flow stage. The poro-elastic stage results from the excavation of the slope in which the slope is unloaded (destressed) and usually occurs rapidly, due to blasting. Typically, time is ignored in the poro-elastic stage. The unloading generally increases the fracture apertures, particularly those near the slope and oriented parallel to the slope. Owing to the low porosity of the rock mass and high bulk modulus of water, water pressures can drop significantly due to poro-elastic effects. In the next stage, the transient flow stage, water flows adjust to the new boundary, and pressure conditions resulting from excavation. The time required for water to flow into areas of low pressure (caused by poro-elastic effects) depends on the conductivity of the rock and amount of water available. Time is an important factor in the transient flow stage in which highly transmissive structures reach steady-state conditions much faster than less transmissive structures.

Illustrative Example

The fundamentals of coupled hydro-mechanical slope behavior can be seen in the following idealized example analyzed using FLAC. The model is 4500-m wide, and the slope height is 1050 m. The slope is composed of homogeneously and isotropically fractured rock, which is modeled as an elastic material. A constant pressure boundary is assumed to exist away from the slope. The material and fluid properties assumed for this problem are listed in Table 2.

Properties	Values
Dry Density (kg/m³)	2650
Bulk Modulus (GPa)	10
Shear Modulus (GPa)	3
Porosity	0.5%
Conductivity (cm/s)	1×10^{-6}
Water Density (kg/m³)	1000
Water Bulk (GPa)	1
Water Tension (Pa)	0

Table II – *Rock and fluid properties for the slope example*

The simulation was run in seven stages, as excavation was assumed to be taken over seven years. Each year a 150-m increment of rock is removed instantaneously. Of particular interest is the behavior of two pressure monitoring points in the slope. One point (A) is located near the slope face and the other (B) is located farther away.

Figure 11 shows the pressure evolution of both points. The histories clearly show the behavior described previously. The point near the slope experiences large instantaneous pressure drops due to slope excavation and slow recovery toward steady- state conditions. The point farther from the slope face experiences less pressure drop and faster recovery. The principles suggested in this hypothetical example are demonstrated more convincingly in a real case example discussed by Galera et al. (38) in this conference.
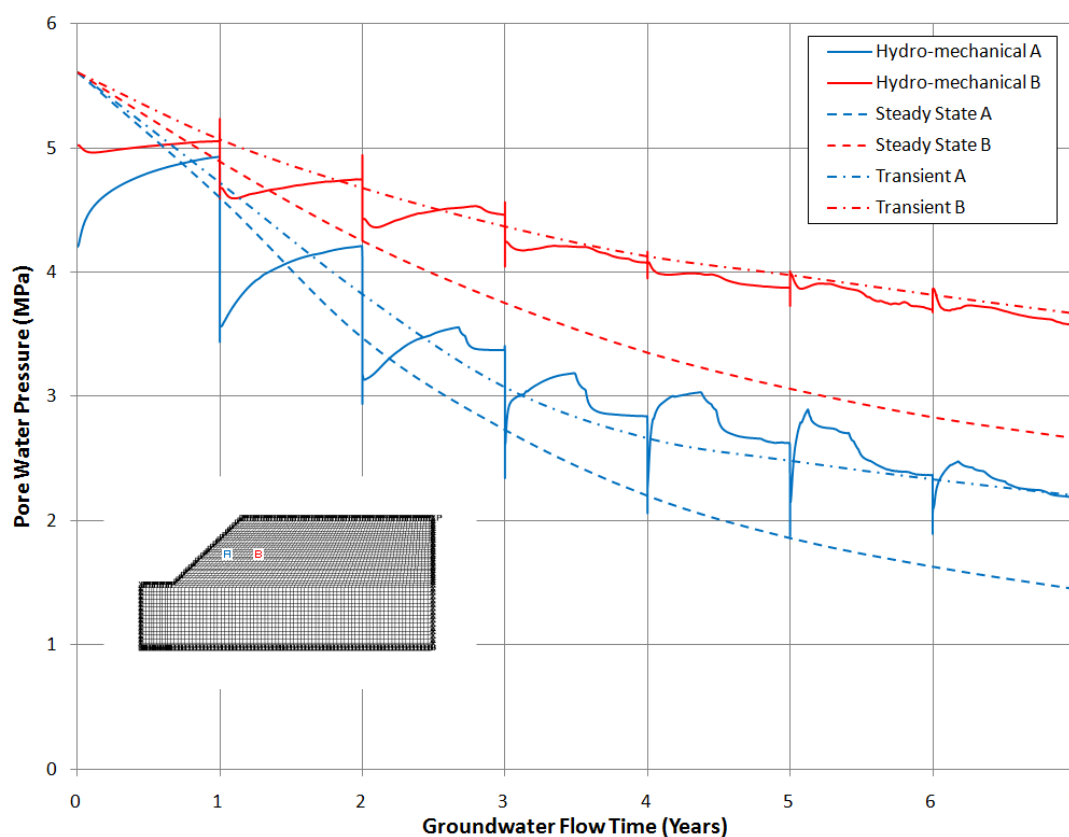
Figure 11 – *Pore pressure evolution at point A (blue line) and point B (red line) versus groundwater flow time (years). Slope is 1050-m high and is assumed to be excavated in seven yearly increments.*

Discussion

In the preceding example, the rock conductivity was assumed to be homogeneous, and conductivity did not change as a result of mechanical effects. The question concerns the differences that would result from a more realistic distribution of hydraulic properties. It seems reasonable to assume that less conductive parts of the rock mass would reach steady-state conditions even slower than shown here. Because typical flow analyses assume homogeneous conductivities, it is possible that water pressures in some parts of the rock mass are over-predicted by flow analyses, particularly if poro-elastic pressure drops are ignored. Because conventional design methods for rock slopes involve the use of continuum strength criteria for the rock mass, in which yield of both intact material and joints must occur, direct application of water pressures from flow analysis is probably misleading.

The characterization of the influence of groundwater pore pressures and flow on the deformation of massive rock slopes represents an important 'missing link', if numerical models of rock slopes are to be understood adequately. The assumption of tenuous water tables and associated pore pressure distribution in fractured rock slopes is an area of considerable model uncertainty (39). This is an area requiring input from both rock mechanics and hydrogeology; it is an area that has been long overlooked and is in need of research attention such as that proposed by the Large Open Pit (LOP) project.

The LOP Project has shown that the SRM approach can be used to significantly reduce uncertainty with respect to rock mass strength. In parallel, it is essential that attention is focused on trying to understand what water pressures should be applied to various components of the rock mass making up the slope. The first part of the research program is aimed at understanding when and if the current equivalent porous media approach can be used, and where it is not appropriate, what methods should be considered.

THE VARIABILITY CHALLENGE

Present rock-slope design practice is to divide a slope into geotechnical units, each of idealized constant properties, with similar idealization of large-scale discontinuities into discrete features of known location and constant properties. This conventional practice is combined with admissible safety factors essentially established by experience (and possibly mandated in code — for example, in the case of rock slopes, the 'Eurocode 7' standard BS EN 1997, Part 12 (40)). The combined investigation, analysis and acceptable safety factors define a calculation methodology. This conventional methodology is beginning to be challenged [e.g., (41)]. The optimum design of a pit requires the determination of the most economic pit limit, which normally results in steep slope angles. In general, as the slope angle becomes steeper, the stripping ratio (waste-to-ore ratio) is reduced, and the mining economics improve. However, these benefits are counteracted by reduced slope stability and the consequent increased risk to the operation. Thus, determination of the acceptable slope angle is a key aspect of a mine's business. Rather than simply accepting a precedent factor of safety, mine owners are beginning to find value in the formal assessment of slope-design reliability — which may indicate that steeper slopes have acceptable reliability. A key part of this process is assessing the effect of rock variability on slope stability.

One approach to determining the effect of rock strength variability on slope stability is to model it explicitly, with the pattern of strengths in the model matching that in the ground. However, as the actual variability of rock properties is known only at the locations of the investigation borings, and from what can be added from mapping surface exposures, there can be many possible patterns of rock strength distribution, each of which honors the site investigation information. This is actually the crux of the problem, as it is an improper distribution-matching of the site data that leads to unexpected slope performance. Thus, repeated simulations are made, and the proportion that leads to a factor of safety (FS) less than 1 indicates the probability of slope failure. (Strictly, there are other factors, including 'model uncertainty' in the analysis method, but the focus here is on ascertaining the contribution from the real variability of rock strength.) This type of approach is referred to as 'stochastic analysis', and it is beginning to be used for soil slopes [e.g.,(42) and (43)]; however, it apparently has not yet been attempted for rock slopes.

In this section, an implementation of stochastic analysis of a rock slope using FLAC (28) is described. This simple analysis is only a first step in determining the significance of property variability on slope performance. Structural features and their variability are neglected; the concentration is on the rock mass. Only one geological unit is considered, thus neglecting the effect of uncertainty in the location of boundaries between various geological units. However, the results are striking. Because this type of analysis is not especially difficult to implement comprehensively, more widespread use of stochastic analysis may be helpful in developing reliable, steeper pit slopes.

Variability of Rock Mass Properties

The ground has intrinsically varying properties from place to place as a consequence of the processes involved in its formation and its subsequent geological history. This shows up in site investigation results when a scatter in properties invariably is found. As an example of this situation, Figure 12 shows a histogram of the results of some 8000 characterizations of the geological strength index (GSI) within a single identified geological unit. These data were taken from a recent site characterization for a large open-pit mine that was unusually comprehensive, but similar patterns arise elsewhere — even with far fewer observations. In fact, other geological units at the mine exhibited similar data; these were adopted simply as a convenient example having a large amount of data. The mean and standard deviations of the GSI data shown on Figure 12 are 48.5 and 11.0, respectively.

The histogram shown on Figure 12 has two components. First, some of the variability found reflects the true variation in the in-situ rock mass. Second, the procedure for determining GSI has some intrinsic scatter. As the precision in this second aspect has not been ascertained in comparative replicate trials, it is assumed that all the variation seen in Figure 12 is actually variation in the ground itself (i.e., assuming no testing error). The objective of the analysis presented here was explicitly to include the pattern of variability seen in Figure

12 within the analyzed domain, with the FLAC model zones having individual GSI (and UCS) values such that 'drilling' a series of boreholes through the model domain would produce something similar to Figure 12.

The average values of the rock mass parameters are chosen such that the safety factor of the slope may be between 0.8 and 1.3. A suitable set of parameters is given by $m_i = 20$, UCS = 40 MPa and GSI = 45. This case produces a safety factor of 1.17.
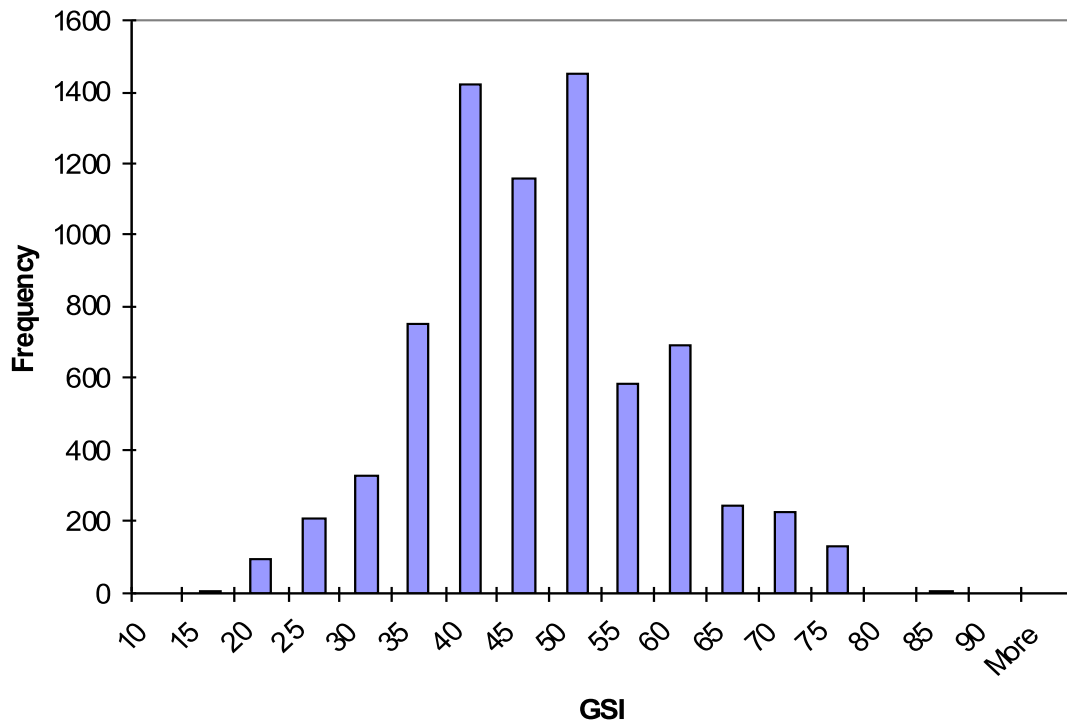
Figure 12 – *Histogram of GSI determinations*

Representing Rock Mass Variability

Various distributions could be fitted to Figure 12, with goodness-of-fit tests to establish which might have the greatest likelihood of being ground truth. However, inspection of the histogram suggests that the familiar normal distribution is a reasonable first approximation. A normal distribution was adopted, but also included a truncation at the low bound to GSI > 10. This was done because the mean and standard deviations of the data shown on Figure 12 lead to a small probability of negative GSI, which is impossible.

Presenting in-situ variability data in the form shown on Figure 12 misses three other important associated parameters: (1) the length scale of fluctuation vertically, (2) the length scale of fluctuation horizontally, and (3) the orientation of the maximum length direction to vertical. Figure 13 shows a slope with strength contoured as a gray scale, maximum strength as black, and least strength as white. Length scale can be viewed as the average distance between adjacent black zones. The orientation is self-evident.

Vertical length scales usually are determined from site investigation data using an auto-correlation process on the borehole (or probing, in the case of soils) data. Determining horizontal length scales is more problematic, as borehole/probing data are needed at spacings much closer than the characteristic length so that an auto-correlation can be carried out horizontally. Few site investigations, even intensive ones, have met this requirement to date. Horizontal characteristic length usually is assumed to be no smaller than vertical, and the effects of anisotropy are explored by parametric simulations. Orientation usually is based on the strata dip.

Figure 13 – *Example of strength distribution in a soil slope (44).*

In the site investigation, determination of the vertical length scale was feasible, and the orientation known for the various geological units. However, this section of the paper is a scoping study, not an analysis of a particular slope, and site-specific data were not used. Rather, four scenarios were adopted to explore the effects of length scale on slope behavior. The scenarios selected for the simulations are shown on Table 3. The distributions for UCS and GSI were assumed to be uncorrelated, an assumption about the nature of rock mass strength that could be considered further.

The stochastic field for the slope was created by first locating cells at half the selected characteristic spacing. The cells adopted for the stochastic field generation were identical to the grid of the FLAC model. The value of GSI then was realized randomly from the specified parent distribution (normal, in this case) at each of these 'independent' cells. The reason for the half-spacing is that an adjacent cell is equally likely to be low rather than high, as assumed in the definition of characteristic length. Linear interpolation then was used to fill in the remaining cells. The mean and standard deviations of this realized distribution were calculated. Finally, all realized values were re-scaled to bring the realized distribution into perfect alignment with the specified mean and standard deviations. This is a first-order procedure, and the element size is also coarse, to represent subtle fluctuations in property variation. Consequently, the realized fields do not display perfect normal distributions. Figure 14 presents a PDF plot of a random example of a realized distribution and the specified normal distribution. Of course, the normal distribution is itself an idealization of the underlying data, and, in some ways, the realized distribution is quite close to the original histogram from the site investigation (Figure 12).

| Scenario	Characteristic Length		Orientation	GSI Distribution	UCS Distribution (as MPa)
	Vertical	Horizontal			
1	50 m	50 m	Horizontal	Normal (45.0, 10.0)	Normal (40.0, 8.0)
2	250 m	250 m	Horizontal	Normal (45.0, 10.0)	Normal (40.0, 8.0)
3	25 m	125 m	Horizontal	Normal (45.0, 10.0)	Normal (40.0, 8.0)
4	50 m	250 m	Horizontal	Normal (45.0, 10.0)	Normal (40.0, 8.0)

**Table III** – *Stochastic property scenarios used in this study*
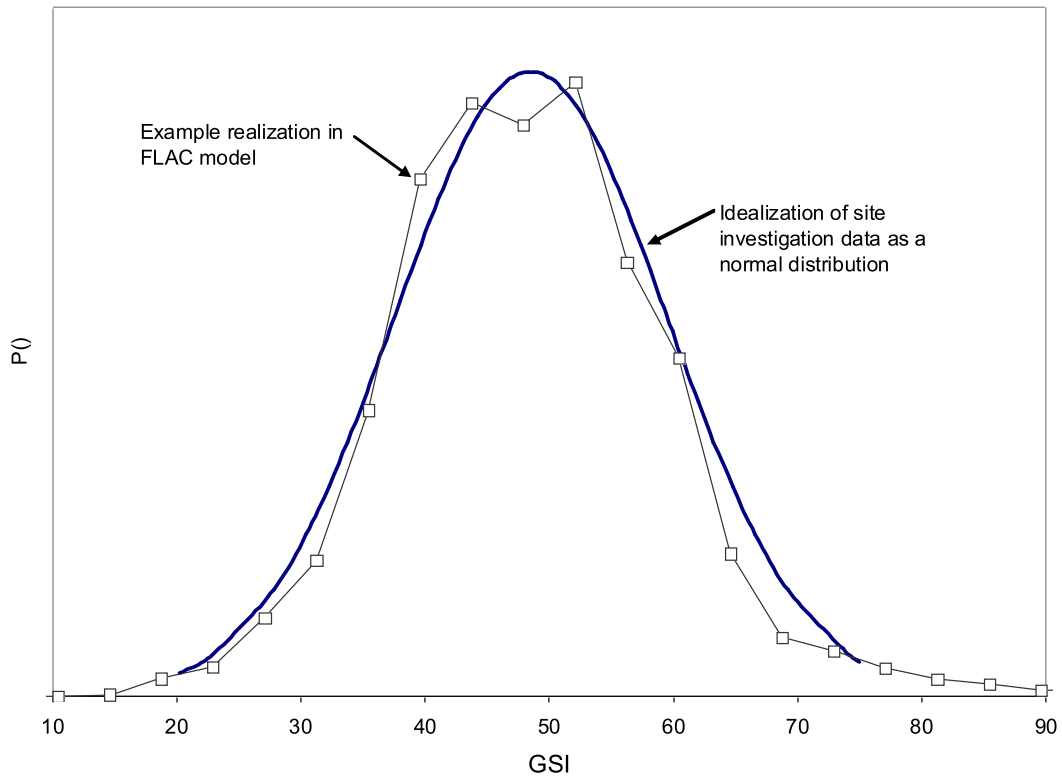
Figure 14 – Comparison of one realized distribution of GSI to the idealized 'ground truth'

Examples of the realized distribution of properties for each of the four scenarios are shown on Figure 15, again using linear gray-scale shading, with GSI = 100 being black and GSI = 0 being white. The effect of length scale and anisotropy on the realized distribution of GSI are readily apparent. Each of these pictures has identical mean and standard deviations and, within the limits of the discretization accuracy illustrated on Figure 14, a normal distribution.
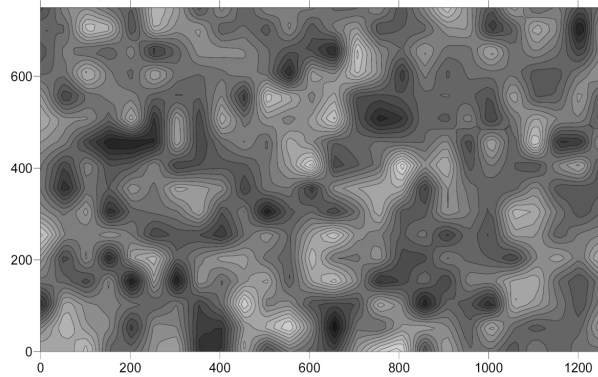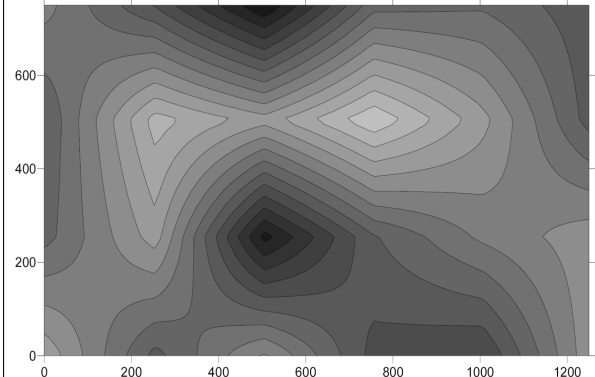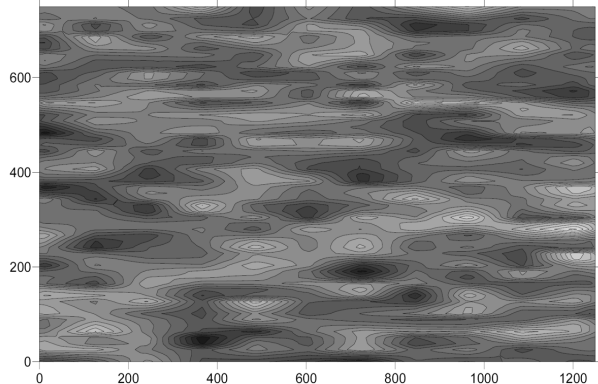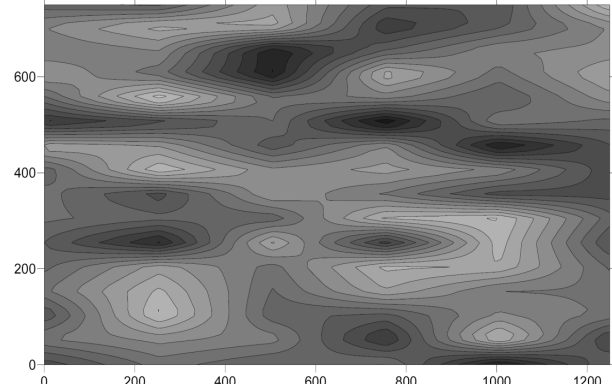

Figure 15 – Four examples illustrating effect of length scale and anisotropy on realized field

Simulation Results

The example problem involved a slope of 500-m height and 45° overall angle. The average values of the rock mass parameters are chosen such that the safety factor of the slope may be between 0.8 and 1.3. A suitable set of parameters is given by $m_i = 20$, UCS = 40 MPa and GSI = 45. This case produces a safety factor of 1.17. Details of the numerical model can be found in (44).

Each of the four scenarios was realized one hundred times, with FLAC simulations carried out on each realization. The results have been reduced to a simple factor of safety (FS) for each realization and are plotted on Figure 16 against the average characteristic length of that scenario. A wide spectrum of FS is found in each scenario, with the range increasing as the average length-scale increases.
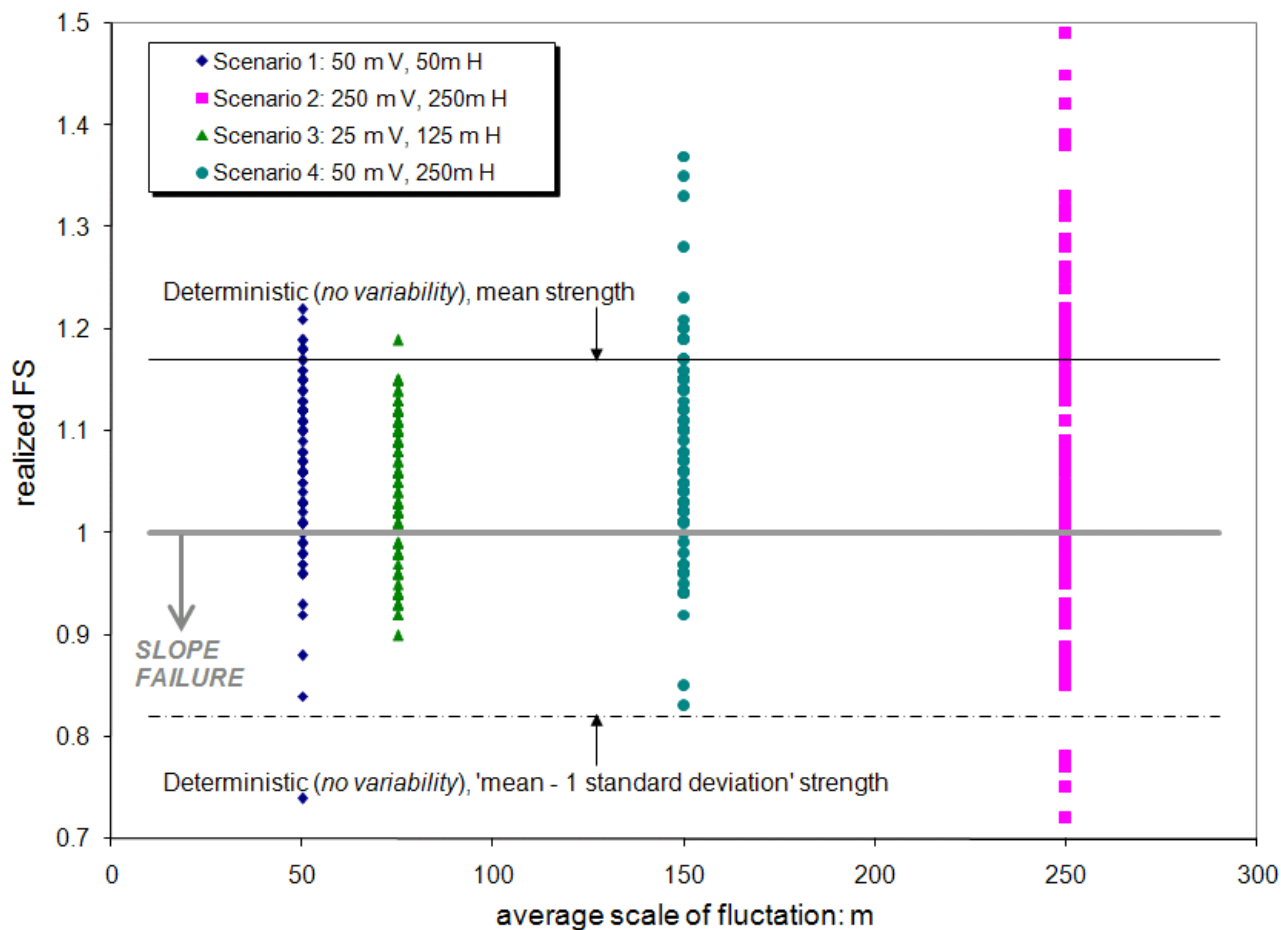

Figure 16 – Results from one hundred realizations of each of the four strength distribution scenarios modeled

Two other results are also shown on Figure 16, both from FLAC simulations using constant properties everywhere (a 'deterministic' case). One result is for GSI = 45 and UCS = 40 MPa, which is the mean strength specified. The second is for a constant GSI = 35 and UCS = 32 MPa, which is the specified mean less one standard deviation — approximately 85% of the ground is stronger than this situation. Because these deterministic simulations have no intrinsic length scale, they have been plotted as horizontal lines against which to compare the stochastic results.

At an average small length scale (less, say, than a quarter of the slope height), the individual stochastic results are all less than the deterministic mean result of FS = 1.17. A line for FS = 1.0 has also been indicated on Figure 14 that can be viewed as the slope failure criterion if model uncertainty is neglected. About 20% of the stochastic simulations result in predicted slope failure, even though the conventional FS = 1.17.

As the length scale is increased, the results depend on whether the realization is predominantly weak or predominantly strong ground. At this point, the limits of the idealization are being pushed, and one expects the site investigation data to show the actual strength in the slope. In essence, if there were a weak or strong zone at length scales of half the slope height (or longer), the domain should be subdivided into additional sub-units of geotechnical behavior rather than relying on stochastic simulation of the entire domain (although each of those sub-units can have their own stochastic strength description).

The results shown above can be used to compute a probability of failure as shown in Figure 17. It is interesting to note that the probability of failures agrees well with an estimated trend based on [(46) and (24)]. The notable exception is the realization based on 250-m characteristic length, which, as noted previously, probably represents different geotechnical domains.

Discussion

This study was triggered by a move toward the probabilistic assessment of slope stability. One component of that probability is the random (or, more accurately, unknowable with current and foreseeable site investigation procedures) spatial distributions of rock mass strength. Using a FLAC analysis of randomly realized distributions of strength, each of which perfectly honors the mean and standard deviations of strength found in data from a large open-pit mine for a slope with a nominal factor of safety of FS = 1.17, there is actually about a one-in-five chance of slope failure. Because of the neglect of brittle failure and other aspects, it is believed this is an under-estimation of the actual situation.

The probability of failure depends on the nominal factor of safety, the spatial distribution of the ground strength, and the variability in that ground strength. This study has been in the nature of an initial scoping to ascertain the credible extent of these factors on slope performance. Further work is needed for a proper understanding of the issues. However, the required analyses are not difficult to implement in FLAC. There would appear to be considerable merit in further use of stochastic methods in slope design.
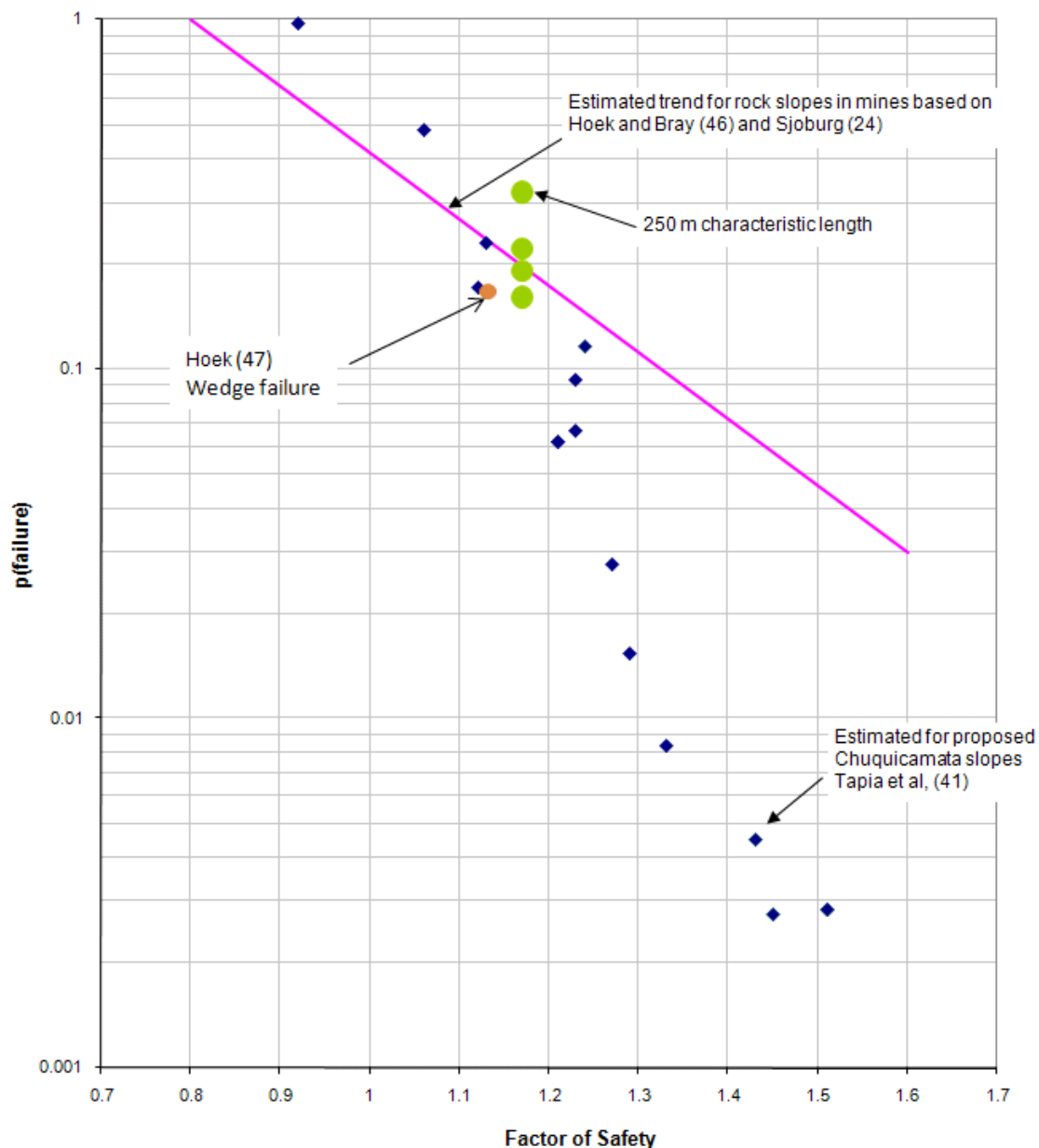

Figure 17 – *Factor of Safety versus Probability of Failure*

CONCLUSIONS

A new generation of numerical models based on a lattice concept eventually will replace current analysis methods. However, considerable testing and application to real problems will be required before they will be used routinely in slope stability analysis. In some sense, this process will parallel the evolution of current continuum and discontinuum models in replacing limit equilibrium methods. In the meantime, however, there is a need to address some of the challenges inherent in current slope stability analysis.

The Synthetic Rock Mass approach is proposed as an appealing method for better understanding and prediction of jointed rock-mass behavior. The methodology, based on the bonded-particle model for rock (47), involves construction of a synthetic 'sample' of the rock mass in three dimensions by bonding together thousands of spherical particles and embedding the fracture network of not-persistent pre-existing joints. The ability of the SRM model to construct an 'equivalent material' that honors the strength of the intact rock and joint fabric that may occur along a candidate failure surface in a closely jointed rock mass is a significant new development. The SRM approach already has been demonstrated to overcome many of the limitations inherent in empirical estimates of rock mass properties. It can provide a means of establishing a constitutive material model (strength envelope) that is not reliant on either Mohr Coulomb or Hoek-Brown criteria, but it can also be used to provide better rock-mass property estimates for use with existing criteria. For example, it can be used estimate rock "block' strengths when the rock blocks exceed the size of laboratory samples, but are smaller than an entire slope.

All slope stability analyses involving water could benefit from better understanding of the hydro-mechanical behavior of slopes, particularly the poro-elastic effects resulting from slope unloading. Most rock slopes appear to have conductivities similar to silts, but with considerably reduced porosity. In the idealized example shown here, the calculated water pressure near the slope based on poro-elastic considerations is much closer to the transient water pressure than the steady-state condition. However, the real issue involves the hydro-mechanical behavior of non-ideal slopes made up of a rock mass with a widely varying conductivity.

The discussion of rock mass variability has shown that rock masses have the ability to find failure paths of least resistance. The larger the rock mass being considered, the greater the number of potential failure paths. This observation leads directly to an understanding of scale effects and explains why larger rock masses have lower overall strength compared to smaller rock masses. Finally, nothing ever fails with average properties. This has implications for characterization and back-analysis, which means that rock mass characterization should focus on trying to identify the weakest parts of the rock mass. It also means that the results of back-analysis do not provide an understanding of the average strength of the rock mass but, rather, strengths that can be considerably less than the average values.

ACKNOWLEDGEMENTS

REFERENCES

1. B. Singh and R.K. Goel, Rock Mass Classification — A Practical Engineering Approach, Elsevier, Oxford, 1999.

2. N. Barton, R. Lien and J. Lunde, "Engineering Classification of Rock Masses for the Design of Tunnel Support", Rock Mechanics, Vol. 6, 1974, 89-236.

3. Z.T. Bieniawski, "Rock Mass Classifications in Rock Engineering", Exploration for Rock Engineering (Johannesburg, November 1976), Balkema, Rotterdam, 1976, 97-106.

4. D.H. Laubscher, "Geomechanics Classification of Jointed Rock Masses — Mining Applications", Transactions Institution of Mining and Metallurgy(a), Vol. 86, 1977, A1-A8.

5. M.J. Selby, "A Rock Mass Strength Classification for Geomorphic Purposes: with Tests from Antarctica and New Zealand", Zeitschrift Geomorphologie, N.F., Vol. 24, No. 1, 1980, 31-51.

6. M. Romana, "New Adjustment Ratings for Application of Bieniawski Classification to Slopes", Proceedings, International Symposium on the Role of Rock Mechanics (Zacatecas), 1985, 49-53.

7. A.M. Robertson, "Estimating Weak Rock Strength", SME Annual Meeting, Phoenix, Arizona, Society of Mining Engineers, 1988, Preprint 88–145.

8. E. Hoek, "Strength of Rock and Rock Masses", ISRM News Journal, Vol. 2. No. 2, 1994, 4-16.

9. Z. Chen, "Recent Developments in Slope Stability Analysis", Proceedings, ISRM International Congress on Rock Mechanics (Tokyo, 1995), Vol. 3, Balkema, Rotterdam, 1995, 1995, 1041-1048.

10. A. Palmstrøm, "Characterizing Rock Masses by the RMi for Use in Practical Rock Engineering, Part 1: The Development of the Rock Mass Index (RMi)", Tunnelling & Underground Space Technology, Vol. 11, No. 3, 1996, 287-303.

11. E. Unal, "Modified Rock Mass Classification: M-RMR System", Milestones in Rock Engineering. The Bieniawski Jubilee Collection, Balkema, Rotterdam, 1996, 203-223.

12. Y. Lin, "An Introduction of the Chinese Standard for Engineering Classification of Rock Mass (GB50218-94)", Advances in Rock Mechanics, Y. Lin, Ed., World Scientific Publishing, Singapore, 1988, 317- 327.

13. E. Hoek and P. Marinos, "A Brief History of the Development of the Hoek-Brown Failure Criterion", Rocscience, http://www.rocscience.com/library, 2007.

14. E. Hoek and E.T. Brown, Underground Excavations in Rock, IMM, London, 1980.

15. E. Hoek, "Strength of Jointed Rock Masses, 23rd Rankine Lecture", Géotechnique, Vol. 33, No. 3, 1983, 187-223.

16. E. Hoek and E.T. Brown, "The Hoek-Brown Failure Criterion — A 1988 Update", Rock Engineering for Underground Excavations, University of Toronto, Dept. of Civil Engineering, Toronto, 1988, 31-38.

17. E. Hoek, D. Wood and S. Shah, "A Modified Hoek-Brown Failure Criterion for Jointed Rock Masses", Rock Characterization (Chester, U.K., September 1992), J.A. Hudson, Ed., British Geotechnical Society, London, 1992, 209-213.

18. E. Hoek and E.T. Brown, "Practical Estimates of Rock Mass Strength", International Journal of Rock Mechanics and Mining Science, Vol. 34, No. 8, 1997, 1165-1186.

19. E. Hoek, C. Carranza-Torres and B. Corkum, "Hoek-Brown Failure Criterion — 2002 Edition", NARMS-TAC 2002: Mining and Tunnelling Innovation and Opportunity, Vol. 1, R. Hammah et al., Eds., University of Toronto Press, Toronto, 2002, 267-273.

20. K.J. Douglas, "The Shear Strength of Rock Masses", Ph.D. Thesis, The University of New South Wales, UK, December 2002.

21. W. Gibson, "Rock Mass Strength from Rock Mass Characterization", Journal of Australian Geomechanics, Vol. 41, No. 1., 2006, 45-51.

22. M. Cai, P.K. Kaiser, H. Uno, Y. Tasaka and M. Minami, "Estimation of Rock Mass Deformation Modulus and Strength of Jointed Hard Rock Masses Using GSI System", International Journal of Rock Mechanics and Mining Science, Vo. 41, 2004, 3-19.

23. P. Cundall, C. Carranza-Torres and R. Hart. "A New Constitutive Model Based on the Hoek-Brown Criterion", FLAC and Numerical Modeling in Geomechanics — 2003, R. Brummer et al., Eds., Balkema, Lisse, 17-25.

24. J. Sjöberg, "Analysis of Large Scale Rock Slopes", Doctoral Thesis 1999:01, Division of Rock Mechanics, Luleå University of Technology, 1999.

25. J.L. Carvalho, D.T. Kennard and L. Lorig, "Numerical Analysis of the East Wall of Toquepala Mine, Southern Andes of Peru", EUROCK 2002 (Medeira, Portugal, November 2002), C. Dinas da Gama and L. Ribeiro e Sousa, Eds., Sociedade Portuguesa de Geotecnica, Lisbon, 2002, 615-625.

26. Itasca Consulting Group, Inc., UDEC (Universal Distinct Element Code), Version 4.0, Minneapolis, 2004.

27. I.H. Clark, "Simulation of Rockmass Strength Using Ubiquitous Joints", 4th International FLAC Symposium on Numerical Modeling in Geomechanics – 2006, R. Hart and P. Varona, Eds., Itasca Consulting Group, Inc., Minneapolis, 2006, Paper 08-07.

28. Itasca Consulting Group, Inc. FLAC (Fast Lagrangian Analysis of Continua), Version 5.0, Minneapolis, 2005.

29. E.-S. Park, C.D. Martin and R. Christiansson, "Numerical Simulation of the Mechanical Behavior of Discontinuous Rock Masses", Numerical modeling in Micromechanics via Particle Methods - 2004 (Kyoto, Japan, October 2004), Y. Shimizu et al., Eds., Balkema, Leiden, 2004, 85-91.

30. Itasca Consulting Group, Inc., PFC2D (Particle Flow Code in 2 Dimensions), Version 3.1, Minneapolis, 2004.

31. M. Pierce, P. Cundall, D. Potyondy and D. Mas Ivars, "A Synthetic Rock Mass Model for Jointed Rock", Rock Mechanics: Meeting Society's Challenges and Demands, Vol. 1: Fundamentals, New Technologies & New Ideas, E. Eberhardt et al., Eds., Taylor & Francis Group, London, 2007, 341-349.

32. N. Barton, TBM Tunneling in Jointed and Faulted Rock, Balkema, Rotterdam, 2000.

33. E. Hoek, "Estimates of Rock Mass Strength and Deformation Modulus", Rocscience, Discussion paper #4, http://www.rocscience.com/library, 2004.

34. P.A. Cundall and B. Damjanac, "A Comprehensive 3D Model for Rock Slopes Based on Micromechanics", to be presented at Rock Slope Stability 2009, Universidad de los Andes, Santiago, Chile, November 9-11, 2009.

35. J.K. Furtney, P.A. Cundall and G.D. Chitombo. "Developments in Numerical Modeling of Blast Induced Rock Fragmentation: Updates from the HSBM Project," to be presented at the 9th International Symposium on Rock Fragmentation by Blasting, Granada, Spain, September 13-17, 2009.

36. L.C. Atkinson, "The Role and Mitigation of Groundwater in Slope Stability," Slope Stability in Surface Mining, W.A. Hustrulid et al., Eds., SME, Littleton, Colorado, 2000, 427-434.

37. Bear, J., Dynamics of Fluids in Porous Media, Dover Publications, New York, 1972.

38. J.M. Galera, J. Montero, C. Perez, L. Vega and P. Varona, "Coupled Hydromechanical Analysis of Cobre Las Cruces Open Pit", to be presented at Rock Slope Stability 2009, Universidad de los Andes, Santiago, Chile, November 9-11, 2009.

39. D. Stead, E. Eberhardt and J.S. Coggan, "Developments in the Characterization of Complex Rock Slope Deformation and Failure Using Numerical Modelling Techniques", Engineering Geology, Vol. 83, No. 1, 2006, 217-235.

40. British Standards Institution, Eurocode 7, Geotechnical Design - General Rules: BS EN 1997-1:2004, 2004.
41. A. Tapia, L.F. Contreras, M.G. Jefferies and O. Steffen. "Risk Evaluation of Slope Failure at the Chuquicamata Mine", Slope Stability 2007, Y. Potvin, Ed., Australian Centre for Geomechanics, Perth, 2007, 477-495.

42. R. Popescu, J.H. Prevost and G. Deodatis, "Effects of Spatial Variability on Soil Liquefaction: Some Design Recommendations," Géotechnique, Vol. 47, 1997, 1019-1036.

43. M.A. Hicks and R. Boughrarou, "Finite Element Analysis of the Nerlerk Underwater Berm Failures," Géotechnique, Vol. 48, 1998, 169-185.

44. C. Onisiphorou, "Stochastic Analysis of Saturated Soils Using Finite Elements", Ph.D. Thesis, University of Manchester, UK, 2000.

45. M. Jefferies, L. Lorig and C. Alvarez, "Influence of Rock-Strength Spatial Variability on Slope Stability", Continuum and Distinct Element Numerical Modeling in Geo-Engineering, R. Hart et al., Eds., Itasca Consulting Group, Inc., Minneapolis, 2008, Paper 05-01.

46. E. Hoek and J.W. Bray, "Rock Slope Engineering", Institution of Mining and Metallurgy, London, 1974.

47. E. Hoek, "Fundamentals of Slope Design", to be presented at Rock Slope Stability 2009, Universidad de los Andes, Santiago, Chile, November 9-11, 2009.

48. D.O. Potyondy and P.A. Cundall, "A Bonded-Particle Model for Rock," International Journal of Rock Mechanics and Mining Science, Vol. 41, No. 8, 2004, 1329-1364.